Numerical Thermal Analysis and Optimization of Multi-Chip LED Module Using Response Surface Methodology and Genetic Algorithm

HONG-YU TANG[1,2], (Student Member, IEEE), HUAI-YU YE[3], (Member, IEEE),
XIAN-PING CHEN[3], (Member, IEEE), CHENG QIAN[2,4], (Member, IEEE),
XUE-JUN FAN[5], (Senior Member, IEEE), AND GUO-QI ZHANG[1], (Fellow, IEEE)

[1]Electronic Components, Technology and Materials, Delft University of Technology, 2628 CD Delft, The Netherlands
[2]Changzhou Institute of Technology Research for Solid State Lighting, Changzhou 213161, China
[3]Key Laboratory of Optoelectronic Technology & Systems, Education Ministry of China, College of Opto-electronic Engineering, Chongqing University, Chongqing 400044, China
[4]State Key Laboratory of Solid State Lighting, Institute of Semiconductors, Chinese Academy of Sciences, Beijing 100083, China
[5]Department of Mechanical Engineering, Lamar University, Beaumont, TX 77710, USA

Corresponding authors: Huai-Yu Ye (h.ye@tudelft.nl) and Guoqi Zhang (g.q.zhang@tudelft.nl)

ABSTRACT In this paper, the heat transfer performance of the multi-chip (MC) LED module is investigated numerically by using a general analytical solution. The configuration of the module is optimized with genetic algorithm (GA) combined with a response surface methodology. The space between chips, the thickness of the metal core printed circuit board (MCPCB), and the thickness of the base plate are considered as three optimal parameters, while the total thermal resistance (R_{tot}) is considered as a single objective function. After optimizing objectives with GA, the optimal design parameters of three types of MC LED modules are determined. The results show that the thickness of MCPCB has a stronger influence on the total thermal resistance than other parameters. In addition, the sensitivity analysis is performed based on the optimum data. It reveals that R_{tot} increases with the increased thickness of MCPCB, and reduces as the space between chips increases. The effect of the thickness of base plate is far less than that of the thickness of MCPCB. After optimization, three types of MC LED modules obtain lower T_j and R_{tot}. Moreover, the optimized modules can emit large luminous energy under high-power input conditions. Therefore, the optimization results are of great significance in the selection of configuration parameters to improve the performance of the MC LED module.

INDEX TERMS Multi-chip LED module, optimization, response surface methodology, genetic algorithm, thermal resistance.

I. INTRODUCTION

Light emitting diodes (LEDs) have been used as LCD back light sources, automotive and general lightings due to their low power consumption, highly directional light emission, fast response time, long lifetime and environmental protection [1]–[5]. To achieve more lumen and lower cost, LEDs have been packaged in multi-chip packaging modules and driven at high current density [6]–[8]. However, there is only about 20% of the input power is transformed into light in the LEDs, the remaining energy is converted to heat [9]–[11]. If such superheat cannot be removed

effectively, high temperature and temperature gradient inside LEDs will not only generate significant stresses along the interfaces [12]–[14] but also accelerate light output degradation and even catastrophic failure [15]–[19]. Thus, thermal management is necessary for a multi-chip LED (MC LED) module to gain a reliable and good performance [20]–[22]. In general, most of the heat generated from LED chips conducts through heat spreader to substrate and finally transfers from heat sink to environment. There exists a large thermal resistance associated with the spreading of heat from a small heat sources to a much larger substrate base [23]. Besides,

LED module with vertical LED chip shows very high thermal resistance of 15 ∼ 30 °C/W [24] due to the low thermal conductivities of substrate (0.3-3 W/mK for metal core printed circuit board (MCPCB) [25]–[27]). What's more, the number of chips [28] and the layout of LED array [29] have significant effects on the overall illumination quality and thermal performance. Therefore, optimizing the layout of chips and the geometry of module are effective and important for enhancing the performance of MC LED module.

There are several approaches to improve the conductive thermal resistance, thermal spreading resistance, and convective thermal resistance of LED module for decreasing the total thermal resistance. To reduce conductive thermal resistance (also called one-dimensional thermal resistance (R_{1D})), the thickness of solder [30], [31], board and dielectric layer [27] of LED module was optimized separately. Moreover, high thermal conductivity materials, such as carbon nanotube [32] and graphene-based nanocomposite [33], [34] were utilized to decrease R_{1D}. For optimizing the thermal spreading resistance, Cheng *et al.* [7] presented an analytical model for optimizing a uniform temperature profile of multichip LED package by changing the chips arrangement on the substrate. Yung *et al.* [29] addressed different placement configuration and different PCB materials to achieve lower LED temperature and higher luminous efficacy. What's more, lots of studies are focus on the optimum design of heat sink/ heat spreader, which can largely reduce the convectional thermal resistance of LED module [21], [35]. All of the above studies reveal that configuration optimization of LED modules is needed.

Indeed, deign of experiment (DOE) and optimization algorithms have been successfully applied for the optimal design of LED module. Jeon *et al.* [36] optimized the hybrid LED package system based on micro machining technology and Taguchi method. Jeong *et al.* [27] presented geometric optimization in a LED module with aluminum nitride insulation plate by using Box-Behnken design method. In addition, many researchers have successfully optimized the plate-fin heat exchangers/ heat sink with genetic algorithm (GA) and response surface methodology (RSM) by considering maximum the total rate of heat transfer and minimum the total annual cost with given constrained condition [37]–[39]. However, few of them optimize the MC LED module by systematically considering the layout of chips and the geometry of module.

In this paper, an effective general analytical solution proposed by Muzychka *et al.* [40] is used to calculate the heat source temperature and thermal resistance in MC LED module. The objective of present work is to study the effects of configuration parameters (space between the LED chips, thickness of MCPCB and base plate) on the heat dissipation performance of MC LED module. The optimization of the geometric parameters by the RSM and GA with the analytical solution are implemented. The thermal performance and luminous efficacy of the MC LED modules are compared before and after optimization.

II. NUMERICAL ANALYSIS

A. NUMERICAL METHOD

Muzychka *et al.* [40] have presented a general analytical solution for a thermal spreading resistance of eccentric heat sources on a rectangular flux channel. The planar rectangular heat source of dimensions c and d is located at the end of a compound heat flux channel. The channel of dimensions a and b consists of two layers having thicknesses t_1 and t_2 and thermal conductivities k_1 and k_2, respectively. The heat flux is cooled along the bottom surface with a uniform heat transfer coefficient h. The lateral boundaries of the heat flux channel are adiabatic. Q is the total thermal flux from the heat source.

The solution is $\theta\ (x, y, z) = T\ (x, y, z) - T_f$, where $T(x, y, z)$ is the layer temperature, and T_f is the heat sink temperature. It can be used to model any number of discrete heat sources on a heat sink. The temperature excess of each heat source in MC LED module can be computed using the following equation evaluated at the surface:

$$\theta_i(x, y, 0) = A_0^i + \sum_{n=1}^{\infty} A_m^i \cos(\lambda x) + \sum_{n=1}^{\infty} A_n^i \cos(\delta y)$$
$$+ \sum_{m=1}^{\infty} \sum_{n=1}^{\infty} A_{mn}^i \cos(\lambda x) \cos(\delta y), \quad (1)$$

where θ_i is the temperature excess for each heat source by itself, $\lambda = m\pi/a$, $\delta = n\pi/b$; The final Fourier coefficients A_m, A_n, and A_{mn} are obtained by taking Fourier series expansions of boundary condition at the surface $z = 0$.

$$A_0 = \frac{Q}{ab}\left(\frac{t_1}{k_1} + \frac{1}{h}\right) \quad (2)$$

$$A_m = \frac{2Q[\sin(\frac{2X_c+c}{2}\lambda_m) - \sin(\frac{2X_c-c}{2}\lambda_m)]}{abck_1\lambda_m^2\Phi(\lambda_m)} \quad (3)$$

$$A_n = \frac{2Q[\sin(\frac{2Y_c+d}{2}\delta_n) - \sin(\frac{2Y_c-d}{2}\delta_n)]}{abdk_1\delta_n^2\Phi(\delta_n)} \quad (4)$$

$$A_{mn} = \frac{16Q\cos(\lambda_m X_c)\sin(\frac{1}{2}\lambda_m c)\cos(\delta_n Y_c)\sin(\frac{1}{2}\delta_n d)}{abcdk_1\beta_{m,n}\lambda_m\delta_n\Phi(\beta_{m,n})} \quad (5)$$

For N discrete heat sources, the surface temperature distribution is given by:

$$T(x, y, 0) - T_f = \sum_{i=1}^{N} \theta_i(x, y, 0) \quad (6)$$

In general, the total resistance is defined as:

$$R_{\text{tot}} = \frac{\overline{\theta}}{Q} = R_{1D} + R_S, \quad (7)$$

where R_{1D} is the one-dimensional thermal resistance and R_s is the thermal spreading resistance. The thermal spreading resistance of the ith heat source is expressed as:

$$R_{s,i} = \frac{T_j - T_f}{Q} - R_{1D} = \frac{\sum_{i=1}^{N} \overline{\theta_i}}{Q} - \frac{1}{ab}\left(\frac{t_1}{k_1} + \frac{t_2}{k_2} + \frac{1}{h}\right) \quad (8)$$
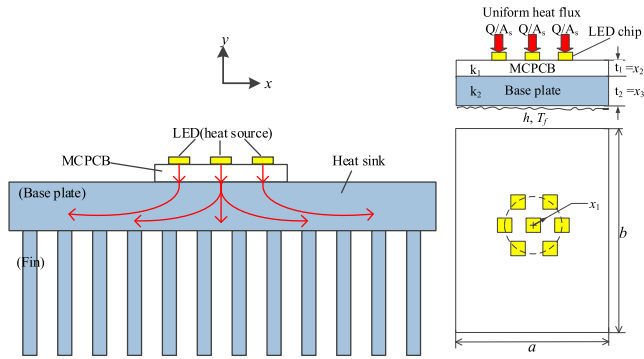
FIGURE 1. Configuration of MC LED module mounted on heat sink (left) and its simplified model (right).

TABLE 1. Values of the geometric and thermal parameters used in the computation.

Layer	Geometry (mm³)	Thermal conductivity (W/mK)
LED chip	1×1×0.1	-
MCPCB	20×26×1.0	4.5
Base plate	20×26×5.0	273

The temperature distribution on the surface of base plate is computed based on the general solution. This paper calculates the maximum thermal resistance in the rectangular flux channels, which is the thermal resistance of heat sources with the highest junction temperature in the MC LED module.

B. MODELING AND NUMERICAL RESULTS

In a LED module, LED chips (heat sources) are bonded on MCPCB (rectangular channel) and mounted on a heat sink (see Fig. 1). The complicated structure of module is simplified to satisfy the condition of the solution presented by Muzychka *et al.*, which consists of a base plate, an MCPCB, and LED chips. LED chips are simplified into squares, whose sizes are 1 mm × 1 mm. The geometric conditions and thermal conductivities of the LED module are listed in Table 1.

An equivalent convection coefficient to represent both the heat transfer in the fin surface and the plate surface is applied on the bottom of base plate, which is 1000 W/m²K here. Since most of heat is dissipated by conduction, heat radiation is neglected here [41]. As shown in Fig. 1, uniform heat flux boundary condition is applied to the top of the chips, while constant temperature condition is applied to the bottom surface of base plate. The heat input Q, calculated by subtracting the light output from the electric power, is 0.28 W. T_f is set as 25 °C. A MATLAB program is built to calculate the above equations (1)-(6) and draw the isothermal chart. A total of 50 terms are used in each of the single and double summations.

One MC LED module, composed of seven LED chips, one MCPCB, and one base plate, is analyzed as shown in Fig. 2. The space between the inner and outer chips is x_1. T_j is the mean junction temperature of the module. Obviously, the T_j
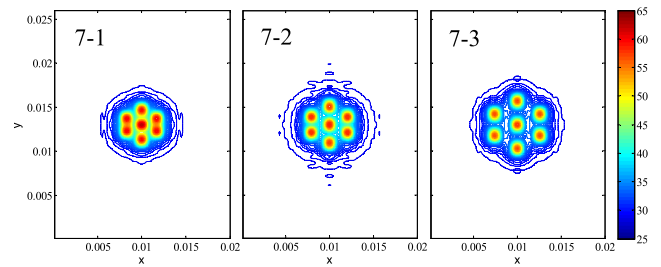

FIGURE 2. Temperature field of the MC LED module by numerical calculation.

drops gradually with increasing x_1. There is no significant change on the edge temperatures of MCPCB (T_{e_c}) because the total thermal power is constant in each module. Likewise, the thermal resistance (R_{tot}) of module decreases with increasing x_1. The results show that the space of the chips has considerable influence on R_{tot} and thermal uniformity of MC LED module. R_{tot} is decreased by nearly 14.5% when the layout changes from the smallest to the largest space between chips.

C. MODEL VALIDATION

For model validation, the numerical results of the present study are compared with the experimental data from three prototypes of the proposed MC LED modules. The T_j of each package with LED chips and MCPCB mounted on a heat sink were measured under room temperature ($T_f = 25$ °C). In our previous work [42], T_j measurements based on the forward voltage method and IR camera [43], [44] were carried out in the experiments. The value of T_j was the average of measured data since the forward voltage measurement was conducted on the LED chips in series.

TABLE 2. The measured and calculated temperature of MC LED module.

No.	T_{j_E} (°C)	T_{e_E} (°C)	R_{tot_E} (°C/W)	T_{j_c} (°C)	T_{e_c} (°C)	R_{tot_c} (°C/W)
7-1	62.75	29.63	16.90	62.78	28.71	17.38
7-2	60.13	29.08	15.84	59.05	28.58	15.55
7-3	57.42	28.25	14.88	57.83	28.71	14.86

Subscripts E and c are for experimental and calculated results respectively.

The thermal resistances of calculation and measurement for MC LED module are listed in Table 2 for comparison. T_{j_E} is the measured mean junction temperature; T_{e_E} is the edge temperature of MCPCB from the experiment. Great thermal resistance and temperature difference on the plate can induce high thermal stress in the interface of the module [1]. Thus, it is necessary to rearrange the space between chips and optimize the configuration of LED module for obtaining lower R_{tot}. As shown in Fig. 3, the calculations are consistent with the experimental data within the accepted error range of 5% in the same configuration and operating conditions. Therefore, the general analytical solutions are available to apply thermal analysis and optimization on the MC LED module.
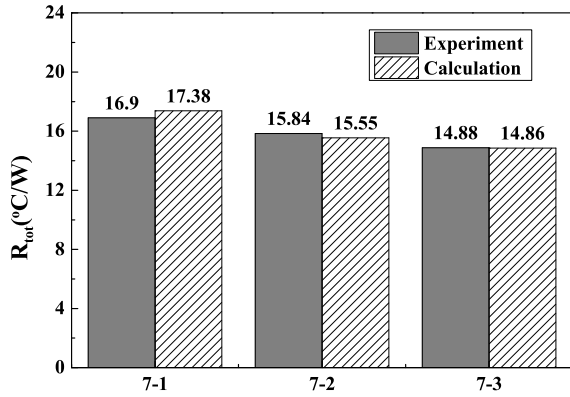
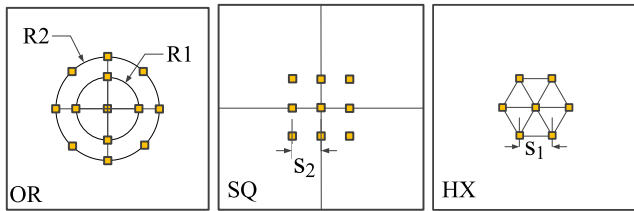**FIGURE 3.** Thermal resistances of calculation and measurement of MC LED module.

FIGURE 4. Schematic of the MC LED module with chips of OR: $2^0 + 2^2 + 2^3 + \ldots + 2^n$ $(n = 3)$ chips, $R_2 - R_1 = R_1 = x_1$, SQ: $n^2 (n = 3)$ $s_2 = x_1$, and HX: $2^0 + 2^1 \times 3 + 2^2 \times 3 + 2^3 \times 3 + \ldots + 2^n \times 3$ $(n = 1)$, $s_1 = x_1$.

III. OPTIMIZATION METHOD

A. THE CONFIGURATION OF MC LED MODULE

To verify the universality of the optimization method presented in this work, three categories typical layouts of MC LED module are selected to perform the heat transfer characteristics, as shown in Fig. 4. The first category, named of OR, is circular distribution with $2^0 + 2^2 + 2^3 + \ldots + 2^n$ $(n = 0, 2, 3 \ldots)$ of the chips. 2^0 chip locates at the center, 2^2 and 2^3 chips are located uniformly in the circle of radius R1 and R2, respectively. 2^n chips are located uniformly in the circle of radius $Rn = n \times R1$. The second category, named of SQ, is squared distribution with $n^2 (n = 2, 3, 4 \ldots)$ of chips. There are n chips in the horizontal and n chips in the vertical. The third category, named of HX, is hexagonal distribution with $2^0 + 2^1 \times 3 + 2^2 \times 3 + 2^3 \times 3 + \ldots + 2^n \times 3$ $(n = 0, 1, 2, 3 \ldots)$ of chips. 2^0 chip locates in the center, $2^1 \times 3$ and $2^2 \times 3$ chips are located uniformly in the hexagon with sides of $1 \times s_1$ and $2 \times s_1$, respectively. 2^n chips are located uniformly in the hexagon with sides of $n \times s_1$. LED chips in those models are simplified into squares with the size of 1 mm × 1mm. According to the actual application, the MCPCB and base plate size is with 50 mm × 50 mm. The space between each adjacent LED (x_1) is changed from 3 mm to 10 mm.

B. OPTIMAL PROCESS

According to Eq. (6) and above discussions, temperature uniformity and thermal resistance of MC LED module show

strong correlation with the layout of the heat source and its configuration. Our aim is to optimize both layout and configuration of the module by minimizing the total thermal resistance R_{tot}. The objective function created by RSM is formulated as

$$y = a_0 + \sum_{i=1}^{n} a_i x_i + \sum_{i=1}^{n} a_{ii} x_i^2 + \sum_{i=1}^{n} \sum_{j=1}^{n} a_{ij} x_i x_j, \quad (9)$$

where a_0, a_i, and a_{ij} are tuning parameters and n is the number of parameters.

As shown in Fig. 1, the considered design parameters in this study are x_1: space between the chip, x_2: thickness of the MCPCB, and x_3: thickness of the base plate. The objective function y denotes R_{tot}. The optimum process is implemented by the combination of RSM and GA, which is shown in Fig. 5 and described as follows.

a) The relationships between the design parameters and objective function are generated by utilizing the Box-Behnken DOE method.

b) Forming RSM, and the goodness of fit is judged by coefficient of determination, root mean square error and relative maximum absolute error, etc.

c) The additional design points would be added to construct new RS, if the above prediction error is larger than 5%. If not, the coefficients of the second order RSM for the objective function are determined by nonlinear regression analysis.

d) Using GA to find out the optimal geometries, which are coded by Matlab toolbox code. The best value of objective function for the initial population is obtained by calculation, and the corresponding chromosome is selected as parent. The initial population size is set as 40. The crossover is selected as scattered and the mutation function is chosen to be 0.001. The crossover combines two chromosomes (parents) to produce a new chromosome (offspring).

e) GA solves the optimization problem iteratively based on the biological evolution process in nature. If the minimum fitness values are low, and fewer offsprings are eliminated, optimization will be stopped by meeting an end criterion.

IV. RESULTS AND DISCUSSION

A. OPTIMIZATION ON THE CONFIGURATION OF THE LED MODEL

According to the preliminary tests and geometric constraints of the LED modules, the ranges of the design parameters are selected as 3 mm $\leq x_1 \leq$ 10 mm; 0.1mm $\leq x_2 \leq$ 2 mm; 1 mm $\leq x_3 \leq$ 5 mm. Numerical simulations of three types for MC LED modules are performed by Matlab through Box-Behnken design. Based on the results in

Table 3, the coefficients of the second-order RSM are determined and given in Table 4.

After optimizing objectives with GA, the optimal design parameters of three types of MC LED modules are

TABLE 3. Results of the Box-Behnken design method for three types of modules.

Design case	x_1	x_2	x_3	$y_{\_OR}$	$y_{\_SQ}$	$y_{\_HX}$
1	3.00	1.05	1.00	7.52	13.35	13.18
2	3.00	0.10	3.00	1.83	3.16	3.18
3	10.00	1.05	5.00	6.68	12.13	12.47
4	10.00	1.05	1.00	6.74	12.27	12.48
5	6.50	1.05	3.00	6.68	11.73	12.12
6	3.00	2.00	3.00	8.33	15.00	15.03
7	6.50	0.10	1.00	1.59	2.96	3.06
8	6.50	1.05	3.00	6.68	11.73	12.12
9	10.00	2.00	3.00	7.43	13.63	13.86
10	3.00	1.05	5.00	7.15	12.73	12.63
11	6.50	1.05	3.00	6.68	11.73	12.12
12	6.50	2.00	1.00	7.38	13.35	13.72
13	6.50	2.00	5.00	7.32	13.08	13.47
14	6.50	0.10	5.00	1.61	2.75	2.91
15	10.00	0.10	3.00	1.60	2.75	2.93

TABLE 4. Coefficients of the second-order RSM for three types of modules.

Coefficient	Value		
	OR	SQ	HX
a_0	2.33412	4.80584	3.77735
a_1	-0.41947	-0.89497	-0.61479
a_2	8.65627	15.1378	15.31265
a_3	-0.10515	-0.40141	-0.25667
a_{12}	-0.05017	-0.071732	-0.06889
a_{13}	0.011227	0.017431	0.01926
a_{23}	-0.01077	-9.38E-03	-0.01288
a_{11}	0.027176	0.061131	0.042108
a_{22}	-2.45802	-4.25218	-4.30246
a_{33}	2.27E-03	0.036716	0.014149

FIGURE 5. Flowchart of the optimization process.

determined as follows: OR: $x_1 = 6.533$ mm, $x_2 = 0.10$ mm, $x_3 = 3.45$ mm, $y = 1.59$ °C/W, $R_s = 1.09$°C/W; SQ: $x_1 = 6.627$ mm, $x_2 = 0.10$ mm, $x_3 = 3.865$ mm, $y = 2.82$ °C/W, $R_s = 2.33$°C/W; HX: $x_1 = 6.365$ mm, $x_2 = 0.10$ mm, $x_3 = 4.765$ mm, $y = 2.84$ °C/W, $R_s = 2.34$°C/W. Therefore, the heat dissipation performances of the modules are estimated based on the determined optimal design parameters.

B. SENSITIVITY ANALYSIS

1) EFFECTS OF DESIGN PARAMETERS

By varying the value of the selected parameter, the effects of each design parameter on the thermal resistance can be discussed. The heat input and the ambient temperature are fixed at 0.28 W per chip and 25 °C, respectively. Fig. 6 shows the effects of design variables on the total thermal resistance.
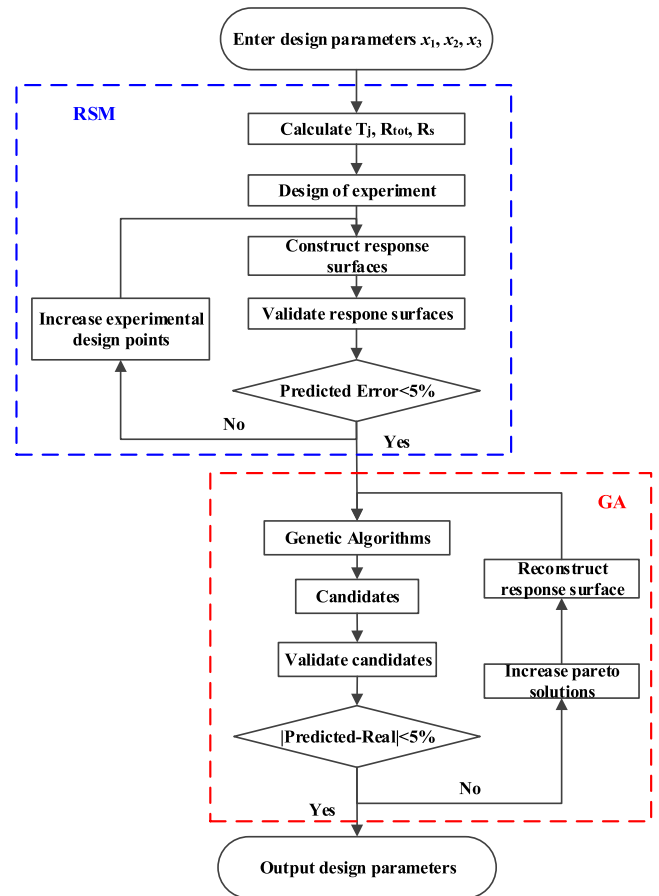
As shown in Fig. 6(a), the R_{tot} of OR and SQ decrease slightly (by ~7%) with increasing x_1. Thus, the optimum x_1 for OR and SQ are determined as 6.533 mm and 6.627 mm, respectively. The R_{tot} of HX decrease until x_1 increase to 6.365 mm, and then increase with increasing x_1. Therefore, increasing the space between the chips is beneficial to improve heat transfer. Fig. 6(b) shows the effects of the MCPCB thickness x_2 on R_{tot}. Obviously, R_{tot} increases rapidly when x_2 is from 0.1 mm to 1 mm and especially in the range of 0.3 mm to 0.5 mm. Therefore, the thickness of MCPCB has negative effects on the improvement of heat transfer. Designer should choose a thinner MCPCB or remove MCPCB from the module. Thus the LED chips is better to be bonded on a base plate with integrated circuit directly. As shown in Fig. 6(c), the effect of x_3 on R_{tot} is relatively small (<7%) compared with that of x_2.

2) SENSITIVITY OF THE GEOMETRIC PARAMETERS

A sensitivity analysis is carried out to determine the optimum mode of the effective parameters on the performance of the module. The sensitivity of the geometric parameters are the derivative of the output variable (y, the minimum thermal resistance) to input parameters (x_1, x_2, x_3), which are
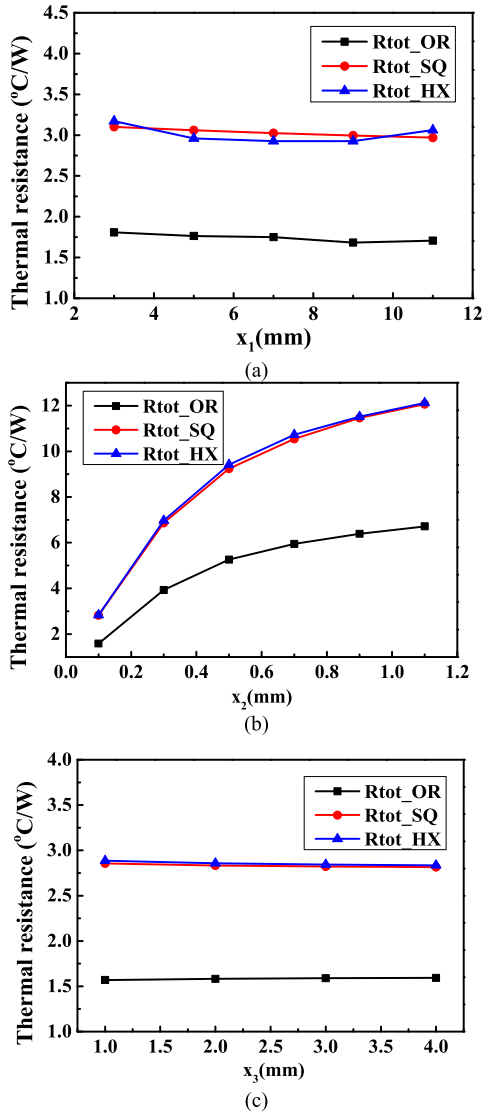
FIGURE 6. Effects of design parameters on R_{tot}. (a) x_1: space between the chip. (b) x_2: thickness of the MCPCB. (c) x_3: thickness of the base plate.

FIGURE 7. Sensitivity of geometric parameters on the objective functions.
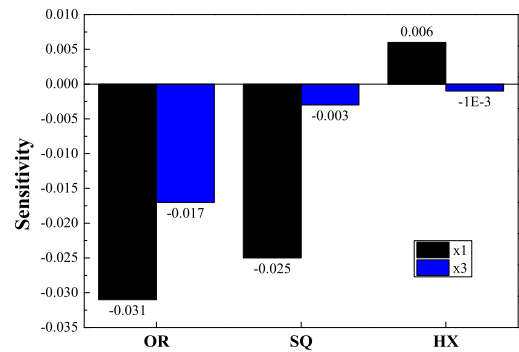
FIGURE 8. Enlarged view of the sensitivity of x_1 and x_3.

calculated as follows:

$$\frac{\partial y}{\partial x_1} = a_1 + a_{12}x_2 + a_{13}x_3 + 2a_{11}x_1 \quad (10)$$

$$\frac{\partial y}{\partial x_2} = a_2 + a_{12}x_1 + a_{23}x_3 + 2a_{22}x_2 \quad (11)$$

$$\frac{\partial y}{\partial x_3} = a_3 + a_{13}x_1 + a_{23}x_2 + 2a_{33}x_3 \quad (12)$$

The positive value of the sensitivity indicates an increase in the objective function with the increasing input parameters, and the negative value represents a reduction. According to the sensitivity results presented in Fig. 7 and Fig. 8, it can be concluded that:

1) The sensitivity of the space between the chips (x_1) for OR and SQ are negative, indicating R_{tot} reduce as x_1 are increased; For HX, the sensitivity of x_1 is positive, which means that R_{tot} increases with increasing x_1. It is
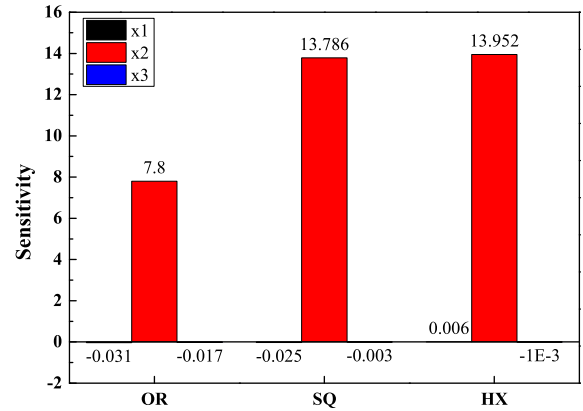
explained why the R_{tot} of HX in Fig. 6(a) first decreases to the trough at $x_1 = 6.365$ mm and then increases as x_1 is increased.

2) The thickness of MCPCB (x_2) has a stronger impact on R_{tot} than x_1 and x_3. The sensitivity of x_2 is positive, which means that the minimum thermal resistance reduces with it. This is fully consistent with the results of Fig. 6(b).

3) The sensitivity of thickness of the base plate (x_3) is negative, indicating that increasing x_3 can reduce the R_{tot}. However, it is far less than that of x_1 and x_2.

4) Overall, the effects of configuration parameters on the thermal performance of MC LED module are studied from qualitatively to quantitatively. All results are of great significance in the selection of geometric parameters of the module to improve its thermal performance.

5) This optimization work is of high efficiency. And it is more available for two-dimensional or equivalent two-dimensional case.

C. THERMAL AND OPTICAL PERFORMANCE OF THE ENHANCED MC LED MODULE

The heat dissipation performance and luminous efficacy of the optimized MC LED modules are compared with that of the original modules ($x_1 = 3$ mm, $x_2 = 1$ mm, $x_3 = 5$ mm). Fig. 9 and Fig. 10 show the temperature
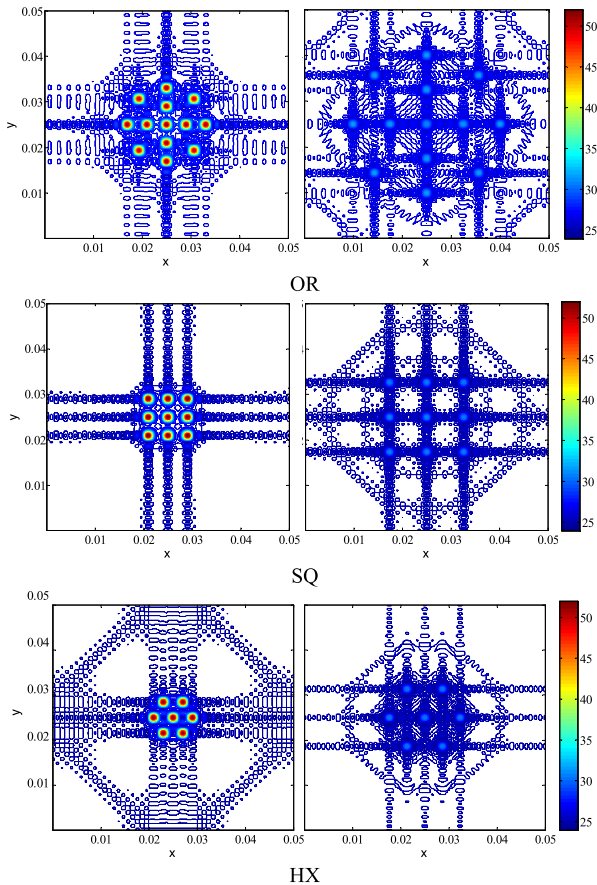
FIGURE 9. Temperature distribution of three types of MC LED modules before (left) and after (right) optimization.
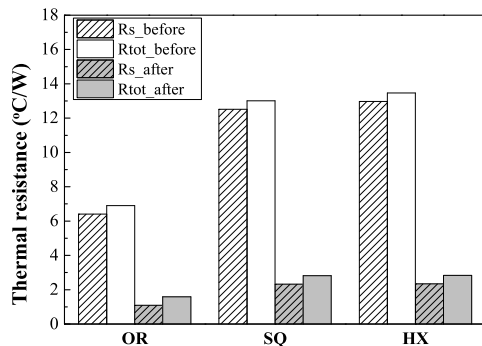

FIGURE 10. Total and spreading thermal resistance of three types of MC LED module before and after optimization.

distribution and thermal resistance of three types of LED modules before and after optimization, respectively. It is obvious that three types of modules obtain lower T_j and R_{tot} after optimization. T_j of each module is decreased by ~62%. R_{tot} of OR, SQ and HX module drop 92.8%, 96.2% and 96.3%, respectively. More uniform temperature distribution leads to lower thermal stress and higher reliability for the module.

The luminous efficacy of the LED module, which was defined as "luminous flux/power consumption" [45], is dependent on the junction temperature of the LED die.
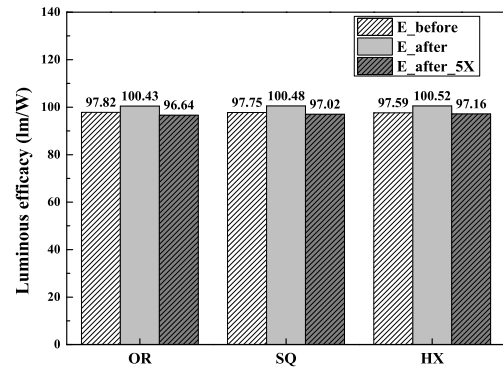

FIGURE 11. Luminous efficacy of three types of MC LED module before and after optimization.

The relationship between the luminous efficacy (E) and junction temperature (T_j) is expressed as follows [46]:

$$E = E_0[1 + k_e(T_j - T_0)], \qquad (13)$$

where E_0 (95.63 lm/W) denotes the rated efficacy at the rated temperature ($T_0 = 64.90$ °C), and k_e is the relative reduction rate of efficacy with increasing temperature. k_e is calculated from the measured luminous efficacy of MC LED module in Section II under different T_j, and is about -0.0015. Fig. 11 shows the luminous efficacy of three types of MC LED modules before and after optimization according to Eq. (13). Also, the T_j and E of the module with 5 times of rated heat input is calculated based on the general analytical solution and optimized model. The result shows that the luminous efficacy decreases slightly under 5 times of rated heat input. It is obvious that the optimized module can allow stable operation under high power input conditions, and emit a large amount of light energy.

V. CONCLUSIONS

In this study, based on the response surface methodology and genetic algorithm, the configuration of MC LED module is optimized. The thermal resistance and temperature distribution of MC LED module with multiple heat sources are calculated by using general analytical solution. The main conclusions are listed as below:

1) The effects of configuration design parameters, including space between chips (x_1) and the thickness of MCPCB (x_2) and base plate (x_3), on thermal resistance (y) are analyzed from qualitatively to quantitatively.

2) After optimizing objectives with GA, the optimal design parameters of three types of modules are determined, verifying the universality of the optimization method presented in this work.

3) The sensitivity analysis is performed based on the optimum data. The results show that x_2 has a stronger impact on R_{tot} than x_1 and x_3. The sensitivity of x_2 is positive, while that of x_1 and x_3 are negative. It indicates that R_{tot} increases with the increased thickness of MCPCB, and reduces as the space between chips

increasing. The effect of the thickness of base plate is slight. Thus, designer should choose a thinner MCPCB, or solder chips on a base plate with integrated circuit directly. Moreover, increasing the space between the chips is beneficial to improve heat transfer.
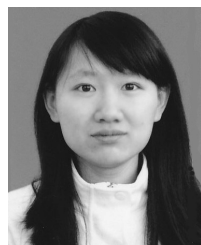
4) Obviously, three types of MC LED modules have lower T_j and R_{tot} after optimization. Encouragingly, the luminous efficacy decreased slightly with increasing T_j and input power, indicating that the optimized module can emit a large amount of light energy under high power input conditions.

The optimization results are of great significance in the selection of geometric parameters to improve the performance of MC LED module with different types of layout.

REFERENCES

[1] W. D. van Driel and X. J. Fan, *Solid State Lighting Reliability: Components to Systems*. Berlin, Germany: Springer-Verlag, 2012.

[2] R. Haitz and J. Y. Tsao, "Solid-state lighting," *Optik Photon.*, vol. 6, no. 2, pp. 26–30, 2011.

[3] S. Pimputkar, J. S. Speck, S. P. DenBaars, and S. Nakamura, "Prospects for LED lighting," *Nature Photon.*, vol. 3, no. 4, pp. 180–182, 2009.

[4] C. Qian, J. Fan, X. Fan, and G. Zhang, "Prediction of lumen depreciation and color shift for phosphor-converted white light-emitting diodes based on a spectral power distribution analysis method," *IEEE Access*, to be published.

[5] M.-H. Chang, D. Das, P. V. Varde, and M. Pecht, "Light emitting diodes reliability review," *Microelectron. Rel.*, vol. 52, no. 5, pp. 762–782, May 2012.

[6] S. Liu and X. Luo, *LED Packaging for Lighting Applications: Design, Manufacturing, and Testing*. New York, NY, USA: Wiley, 2011.

[7] T. Cheng, X. Luo, S. Huang, and S. Liu, "Thermal analysis and optimization of multiple LED packaging based on a general analytical solution," *Int. J. Thermal Sci.*, vol. 49, no. 1, pp. 196–201, 2010.

[8] M. S. Ha, "Thermal analysis of high power LED arrays," M.S. thesis, School Mech. Eng., Georgia Inst. Technol., Atlanta, GA, USA, 2009.

[9] J. Li, F. Lin, D. Wang, and W. Tian, "A loop-heat-pipe heat sink with parallel condensers for high-power integrated LED chips," *Appl. Thermal Eng.*, vol. 56, nos. 1–2, pp. 18–26, Jul. 2013.

[10] X.-Y. Lu, T.-C. Hua, M.-J. Liu, and Y.-X. Cheng, "Thermal analysis of loop heat pipe used for high-power LED," *Thermochim. Acta*, vol. 493, nos. 1–2, pp. 25–29, 2009.

[11] Y. Zhao *et al.*, "Improving peak-wavelength method to measure junction temperature by dual-wavelength LEDs," *IEEE Access*, vol. 5, pp. 11712–11716, 2017.

[12] S.-L. Chuang, A. Ishibashi, S. Kijima, N. Nakayama, M. Ukita, and S. Taniguchi, "Kinetic model for degradation of light-emitting diodes," *IEEE J. Quantum Electron.*, vol. 33, no. 6, pp. 970–979, Jun. 1997.

[13] J. Fan, K.-C. Yung, and M. Pecht, "Lifetime estimation of high-power white LED using degradation-data-driven method," *IEEE Trans. Device Mater. Rel.*, vol. 12, no. 2, pp. 470–477, Jun. 2012.

[14] J. Fan, K.-C. Yung, and M. Pecht, "Prognostics of chromaticity state for phosphor-converted white light emitting diodes using an unscented Kalman filter approach," *IEEE Trans. Device Mater. Rel.*, vol. 14, no. 1, pp. 564–573, Mar. 2014.

[15] J. Fan, K. C. Yung, and M. Pecht, "Physics-of-failure-based prognostics and health management for high-power white light-emitting diode lighting," *IEEE Trans. Device Mater. Rel.*, vol. 11, no. 3, pp. 407–416, Sep. 2011.

[16] J. Xie and M. Pecht, "Reliability prediction modeling of semiconductor light emitting device," *IEEE Trans. Device Mater. Rel.*, vol. 3, no. 4, pp. 218–222, Dec. 2003.

[17] M.-H. Chang, C. Chen, D. Das, and M. Pecht, "Anomaly detection of light-emitting diodes using the similarity-based metric test," *IEEE Trans. Ind. Informat.*, vol. 10, no. 3, pp. 1852–1863, Aug. 2014.

[18] J. Fan, C. Yu, C. Qian, X. Fan, and G. Zhang, "Thermal/luminescence characterization and degradation mechanism analysis on phosphor-converted white LED chip scale packages," *Microelectron. Rel.*, vol. 74, pp. 179–185, Jul. 2017.

[19] C. Qian *et al.*, "Studies of the light output properties for a GaN based blue LED using an electro-optical simulation method," *Microelectron. Rel.*, vol. 74, pp. 173–178, Jul. 2017.

[20] B. Sun *et al.*, "A novel lifetime prediction for integrated LED lamps by electronic-thermal simulation," *Rel. Eng. Syst. Safety*, vol. 163, pp. 14–21, Jul. 2017.

[21] J. Fan, C. Qian, K.-C. Yung, X. Fan, G. Zhang, and M. Pecht, "Optimal design of life testing for high-brightness white LEDs using the six sigma DMAIC approach," *IEEE Trans. Device Mater. Rel.*, vol. 15, no. 4, pp. 576–587, Dec. 2015.

[22] J. Huang *et al.*, "Lumen degradation modeling of white-light LEDs in step stress accelerated degradation test," *Rel. Eng. Syst. Safety*, vol. 154, pp. 152–159, Oct. 2016.

[23] A. Bejan and A. D. Kraus, *Heat Transfer Handbook*. New York, NY, USA: Wiley, 2003.

[24] M. Ha and S. Graham, "Development of a thermal resistance model for chip-on-board packaging of high power LED arrays," *Microelectron. Rel.*, vol. 52, no. 5, pp. 836–844, 2012.

[25] L. Yang, J. Hu, S. Jang, and M. W. Shin, "Thermal design of ceramic packages for high power light-emitting diodes," *Semicond. Sci. Technol.*, vol. 22, no. 7, pp. 705–708, 2007.

[26] B. Pardo *et al.*, "Thermal resistance investigations on new leadframe-based LED packages and boards," *Microelectron. Rel.*, vol. 53, no. 8, pp. 1084–1094, Aug. 2013.

[27] M. W. Jeong, S. W. Jeon, S. H. Lee, and Y. Kim, "Effective heat dissipation and geometric optimization in an LED module with aluminum nitride (AlN) insulation plate," *Appl. Thermal Eng.*, vol. 76, pp. 212–219, Feb. 2015.

[28] L. Kim and M. W. Shin, "Thermal analysis and design of high-power LED packages and systems," *Proc. SPIE*, vol. 6337, p. 63370U, Sep. 2006.

[29] K. C. Yung, H. Liem, and H. S. Choy, "Heat transfer analysis of a high-brightness LED array on PCB under different placement configurations," *Int. Commun. Heat Mass Transf.*, vol. 53, pp. 79–86, Apr. 2014.

[30] K. M. Chen and T. S. Lin, "Copper pillar bump design optimization for lead free flip-chip packaging," *J. Mater. Sci., Mater. Electron.*, vol. 21, no. 3, pp. 278–284, 2009.

[31] X. J. Fan, B. Varia, and Q. Han, "Design and optimization of thermo-mechanical reliability in wafer level packaging," *Microelectron. Rel.*, vol. 50, no. 4, pp. 536–546, 2010.

[32] C.-W. Nan, G. Liu, Y. Lin, and M. Li, "Interface effect on thermal conductivity of carbon nanotube composites," *Appl. Phys. Lett.*, vol. 85, no. 16, pp. 3549–3551, 2004.

[33] S. Lee, J.-Y. Hong, and J. Jang, "Multifunctional graphene sheets embedded in silicone encapsulant for superior performance of light-emitting diodes," *ACS Nano*, vol. 7, no. 7, pp. 5784–5790, 2013.

[34] A. A. Balandin *et al.*, "Superior thermal conductivity of single-layer graphene," *Nano Lett.*, vol. 8, no. 3, pp. 902–907, 2008.

[35] X. R. Meng, X. L. Ma, J. F. Lu, and X. L. Wei, "A study on improving in natural convection heat transfer for heat sink of high power LEDs," *Adv. Mater. Res.*, vols. 383–390, pp. 6834–6839, Nov. 2012.

[36] E.-C. Jeon *et al.*, "Optimization of hybrid LED package system for energy saving based on micro machining technology and Taguchi method," *Int. J. Precis. Eng. Manuf.*, vol. 14, no. 6, pp. 1113–1116, 2013.

[37] J. Wen, H. Yang, X. Tong, K. Li, S. Wang, and Y. Li, "Optimization investigation on configuration parameters of serrated fin in plate-fin heat exchanger using genetic algorithm," *Int. J. Thermal Sci.*, vol. 101, pp. 116–125, Mar. 2016.

[38] M. W. Jeong, S. W. Jeon, and Y. Kim, "Optimal thermal design of a horizontal fin heat sink with a modified-opening model mounted on an LED module," *Appl. Thermal Eng.*, vol. 91, pp. 105–115, Dec. 2015.

[39] K. M. Shirvan, S. Mirzakhanlari, M. Mamourian, and S. A. Kalogirou, "Optimization of effective parameters on solar updraft tower to achieve potential maximum power output: A sensitivity analysis and numerical simulation," *Appl. Energy*, vol. 195, pp. 725–737, Jun. 2017.

[40] Y. S. Muzychka, J. R. Culham, and M. M. Yovanovich, "Thermal spreading resistance of eccentric heat sources on rectangular flux channels," *J. Electron. Packag.*, vol. 125, no. 2, pp. 178–185, 2003.

[41] A. Christensen and S. Graham, "Thermal effects in packaging high power light emitting diode arrays," *Appl. Thermal Eng.*, vol. 29, pp. 364–371, Feb. 2009.

[42] H. Ye, H. Tang, S. Leung, C. Qian, X. Fan, and G. Zhang, "Junction temperature measurement to optimize thermal design of LED arrays," in *Proc. 12th China Int. Forum Solid State Lighting (SSLCHINA)*, Nov. 2015, pp. 47–51.

[43] A. Keppens, W. R. Ryckaert, G. Deconinck, and P. Hanselaer, "High power light-emitting diode junction temperature determination from current-voltage characteristics," *J. Appl. Phys.*, vol. 104, no. 9, p. 093104, 2008.

[44] H. Ye, X. Chen, H. van Zeijl, A. W. J. Gielen, and G. Zhang, "Thermal transient effect and improved junction temperature measurement method in high-voltage light-emitting diodes," *IEEE Electron Device Lett.*, vol. 34, no. 9, pp. 1172–1174, Sep. 2013.

[45] *Guidelines for Combining CIE 127-2007, Total Flux Measurements with Thermal Measurements of LEDs With Exposed Cooling Surface*, document JESD51-52, JEDEC, 2012.

[46] S. Y. Hui and Y. X. Qin, "A general photo-electro-thermal theory for light emitting diode (LED) systems," *IEEE Trans. Power Electron.*, vol. 24, no. 8, pp. 1967–1976, Aug. 2009.

HONG-YU TANG (S'16) received the B.S. and M.S. degrees in microelectronic packaging technology from Guilin University of Electronic Technology, Guilin, China, in 2010 and 2013, respectively. She is currently pursuing the Ph.D. degree with the Faculty of Electrical Engineering Mathematics and Computer Science, Delft University of Technology, Delft, The Netherlands. Her current research interests include the thermal management of high-power devices, and advanced material (micro-/nano- material) applications.

HUAI-YU YE (M'16) received the B.S. degree from Shanghai Jiao Tong University, China, and the M.A. and Ph.D. degrees from Delft University of Technology, The Netherlands. He was with the Materials Innovation Institute and Netherlands Organization for Applied Scientific Research as a Researcher from 2010 to 2014. Since 2014, he has been with Delft University of Technology as a Senior Researcher. He is currently a full-time Professor with Key Laboratory of Optoelectronic Technology and Systems, Education Ministry of China, and the College of Optoelectronic Engineering, Chongqing University, China. His research interests include temperature sensors, computational fluid dynamics in MEMS, thermal management in high-power density electronic devices, microscale/nanoscale nonequilibrium thermodynamics, and microscale/nanoscale energy transport and conversion. He received the One-Hundred Talent Program Scholars of Chongqing University in 2016.

XIAN-PING CHEN (M'15) received the B.Eng. degree from Chongqing University (CQU), China, the M.Sc. degree from Dresden University of Technology, Germany, and the Ph.D. degree from Delft University of Technology, The Netherlands. He was Postdoctoral Researcher with Tsinghua University, China, for two-years. He is currently a full-time Professor with the College of Optoelectronic Engineering, CQU. He is also the Distinguished Expert of Chongqing Municipality, China, and the Technical Committee Member of China Advanced Semiconductor Industry Innovation Alliance. He published about 80 technical papers (over 50 SCI journal publications) and four books. He holds 41 patents. His research interests include electronic materials, electronic packaging, chemical and biological sensors, LED, and nanodevices. He received the One-Hundred Talent Program Scholars of Guangxi in 2013 and the One-Hundred Talent Program Scholars of Chongqing Municipality in 2016, respectively.

CHENG QIAN (M'16) received the B.S. and M.S. degrees in materials science and technology from Beijing Institute of Technology in 2003 and 2006, and the Ph.D. degree in aerospace engineering from Delft University of Technology in 2013. After that, he joined the Changzhou Institute of Technology Research for Solid State Lighting, China. Since 2014, he started his postdoctoral fellowship with the State Key Laboratory of Solid State Lighting, Institute of Semiconductors, Chinese Academy of Science. His current work covers multiple subjects, including LED package/luminaire failure analysis and simulations, development of accelerating test techniques for LED luminaires, lifetime predictions on photonic, and chromatic parameters of the LED package/luminaire. His research interests include the designing reliability of LED luminaires and systems using the combined knowledge of multiphysics numerical simulations and statistical theories.

XUE-JUN FAN (SM'06) received the B.S. and M.S. degrees in applied mechanics from Tianjin University, Tianjin, China, in 1984 and 1986, respectively, and the Ph.D. degree in solid mechanics from Tsinghua University, Beijing, China, in 1989.

In his earlier career, he was promoted to a Full Professor at age 27 in 1991 with the Taiyuan University of Technology, Shanxi, China, and became one of the youngest full professors in China at that time. He was a Senior Staff Engineer with Intel Cooperation, Chandler, AZ, USA, from 2004 to 2007, a Senior Member Research Staff with Philips Research Laboratory, Briarcliff Manor, NY, USA, from 2001 to 2004, and a Member Technical Staff and Group Leader with the Institute of Microelectronics, Singapore, from 1997 to 2000. He is currently a Professor with the Department of Mechanical Engineering, Lamar University, Beaumont, TX, USA, and also a Visiting Professor with the State Key Laboratory of Solid State Lighting, China. His current research interests include design, modeling, material characterization, and reliability in heterogeneous electronic systems.

He has authored more than 200 technical papers, many book chapters, and three books, and holds several patents. He received the IEEE Components Packaging and Manufacturing Technology (CPMT) Society Exceptional Technical Achievement Award in 2011, and the Best Paper Award of the IEEE Transactions on Components and Packaging Technologies in 2009. He is an IEEE CPMT Distinguished Lecturer.

GUO-QI ZHANG (M'03–F'14) received the Ph.D. degree in aerospace engineering from Delft University of Technology, Delft, The Netherlands, in 1993.

Since 2013, he has been a Chair Professor with the Department of Microelectronics, Delft University of Technology. He had been with Philips for 20 years as the Principal Scientist from 1994 to 1996, the Technology Domain Manager from 1996 to 2005, the Senior Director of Technology Strategy from 2005 to 2009, and a Philips Fellow from 2009 to 2013. He also had part-time appointments as a Professor with the Technical University of Eindhoven, The Netherlands, from 2002 to 2005, and as a Chair Professor with Delft University of Technology from 2005 to 2013. He is one of the pioneers in developing the More than Moore (MtM) strategy when he served as a Chair of the MtM Technology Team of European's Nanoelectronics Platform in 2005. He has authored more than 400 papers, including over 150 journal papers, and three books, and 17 book chapters. He holds more than 100 patents. His research interests include heterogeneous micro/nanoelectronics packaging, system integration, and reliability. He received the Outstanding Contributions to Reliability Research Award from the European Center for Micro/Nanoreliability, in 2007, the Excellent Leadership Award at EuroSimE, the Special Achievement Award at ICEPT, and the IEEE Components, Packaging, and Manufacturing Technology Society Outstanding Sustained Technical Contribution Award in 2015.

● ● ●